Second-harmonic generation circular dichroism spectroscopy from tripod-like chiral molecular films*

Wang Xiao-Ou(王晓鸥)†, Chen Li-An(陈立安), Chen Li-Xue(陈历学), Sun Xiu-Dong(孙秀冬), Li Jun-Qing(李俊庆), and Li Chun-Fei(李淳飞)

Department of Physics, Harbin Institute of Technology, Harbin 150001, *China*

(Received 23 February 2010; revised manuscript received 11 April 2010)

The second-harmonic generation (SHG) circular dichroism in the light of reflection from chiral films of tripod-like chiral molecules is investigated. The expressions of the second-harmonic generation circular dichroism are derived from our presented three-coupled-oscillator model for the tripod-like chiral molecules. Spectral dependence of the circular dichroism of SHG from film surface composed of tripod-like chiral molecules is simulated numerically and analysed. Influence of chiral parameters on the second-harmonic generation circular dichroism spectrum in chiral films is studied. The result shows that the second-harmonic generation circular dichroism is a sensitive method of detecting chirality compared with the ordinary circular dichroism in linear optics. All of our work indicates that the classical molecular models are very effective to explain the second-harmonic generation circular dichroism of chiral molecular system. The classical molecular model theory can give us a clear physical picture and brings us very instructive information about the link between the molecular configuration and the nonlinear processes.

Keywords: circular dichroism, three-coupled-oscillator model, tripod-like structure, second-harmonic generation circular dichroism

PACC: 4265B, 4265K, 7820B, 7820E

1. Introduction

Because of their inherent noncentrosymmetry, chiral molecular media show that second-order nonlinear effects concerning the polarization have attracted a great deal of attention of investigators from various fields such as synthesis of asymmetric chemical species, separation of chiral compounds, crystal growth, and the adsorption of proteins at interfaces. It has recently become a hot spot of material physics and material chemistry to design and synthesize, theoretically and experimentally, molecular materials with large nonlinear polarizability.[1−4]

Chiral molecules have different efficiencies in generating the second-harmonic light for left- and right-handed circularly-polarized fundamental beams. This effect is called second-harmonic generation circular-dichroism (SHG-CD). The experiment shows the fact that the SHG-CD effect is several orders of magnitude higher than ordinary circular-dichroism (CD) in linear optics[5] and has closer relation with molecular structure.[6] So the technique has been widely used for measuring chirality from medium films.[7−10] The methodology described provides a formalism conducible to the extraction of structural information from nonlinear optical measurements of chiral films.

The classical models of chiral molecules are often used for studying the second harmonic generation,[11−16] which has a clear physical picture to explain the optical nonlinearity in different chiral molecular systems. In the present paper, we use a new three-coupled-oscillator model[15] to study the SHG-CD in the isotropic thin films composed of chiral molecules with a tripod-like structure in the direction of reflected light. In Section 2, the hyperpolarizabilities of the tripod-like chiral molecules under the condition of second harmonic generation are investigated, and the expressions of surface SHG-CD for tripod-like chiral molecular films are presented. In Section 3, the relation between SHG-CD and molecular microscopic parameters, when the incident light intensity is determinate, will be simulated numerically. The influence of chiral parameters on SHG-CD spectrum in tripod-like chiral molecular films and the spectral dependences of *s*- and *p*-polarized SHG from thin film for left- and right-handed circularly polarized incident light are investigated.

*Project supported by the excellent Team in Harbin Institute of Technology, China, and the Natural Science Foundation of Heilongjiang Province, China (Grant No. A200406).

†Corresponding author. E-mail: wxo@hit.edu.cn

© 2010 Chinese Physical Society and IOP Publishing Ltd

2. Basic theory

The ordinary CD in linear optics is to measure a difference in absorbance of optically active molecules between left- and right-handed circularly polarized light, which may be expressed as a difference in molar extinction coefficients, i.e., $\Delta\varepsilon$ ($\Delta\varepsilon = \varepsilon_{\rm L} - \varepsilon_{\rm R}$), for dilute samples. Usually, ordinary CD spectroscopy relies on a very small rotational strength R, which results from a very weak interaction between the electric and the magnetic dipole transition moments within a molecule. A measure of the SHG-CD intensity asymmetry can be defined as

$$I_{\rm SHG-CD} = \frac{2(I_{\rm left}^{\rm SHG} - I_{\rm right}^{\rm SHG})}{I_{\rm left}^{\rm SHG} + I_{\rm right}^{\rm SHG}}. \quad (1)$$

The intensity of the second-harmonic light generated by a surface can always be expressed in the general form

$$I(2\omega) = \left| fE_p^2(\omega) + gE_s^2(\omega) + hE_p(\omega)E_s(\omega) \right|^2, \quad (2)$$

where $E_p(\omega)$ and $E_s(\omega)$ are respectively the p- and s-polarized components of the fundamental field incident on the surface (see Fig. 1); the coefficients f, g, and h are linear combinations of the various components of the second-order susceptibility tensor $\boldsymbol{\chi}^{(2)}$, which are complex valued,[17] and they are different for the p- and s-polarized second harmonics; $\boldsymbol{\chi}^{(2)}$ is a tensor determined by (we apply the Einstein summation convention)

$$P_I^{(2)} = \varepsilon_0 \chi_{IJK}^{(2)} E_J(\omega) E_K(\omega), \quad (3)$$

where the indices I, J and K refer to the Cartesian laboratory coordinates and may be assigned to X, Y and Z. The tensor $\boldsymbol{\chi}^{(2)}$ is macroscopic polarizability, which is related to the hyperpolarizability $\boldsymbol{\beta}^{(2)}$ of single molecule or molecular group. For the second-order nonlinear process in isotropic chiral film, the macroscopic tensor elements $\chi_{IJK}^{(2)}$ are related to the microscopic parameters of the interfaces, and thus to the information about, such as, the chirality and the orientation of individual molecules. In the electric dipole approximation the macroscopic susceptibility tensor $\boldsymbol{\chi}^{(2)}$ can be correspondingly written as the orientationally averaged microscopic nonlinear polarizability $\beta^{(2)}$ of the surface molecules, i.e.[18]

$$\chi_{IJK}^{(2)} = N f_{\rm L}^3 \left\langle (I \cdot i)(J \cdot j)(K \cdot k) \right\rangle \beta_{ijk}^{(2)}, \quad (4)$$

where i, j, k and I, J, K refer to the molecular and the laboratory frames, respectively; $\langle\ \rangle$ represents the averaging operation of orientation cosines over all possible directions; N is the molecular surface density; f_L^3 is the local field factor of modifications in three directions. The $\boldsymbol{\chi}^{(2)}$ tensor is thus a function of the molecular hyperpolarizability and the orientation of the molecule at the surface. Molecular orientations at surfaces of liquids and polycrystalline solids are usually random with respect to rotations in the plane. For such surfaces, the net macroscopic nonlinear susceptibility must also be invariant with rotations about the perpendicular z-axis. We assume that the orientational z-axis of chiral molecules is arbitrary, whereas the angle θ between the z-axis and the surface normal, which is perpendicular to the film surface, is fixed (see Fig. 1). Here, the 27 elements of the third rank tensor $\boldsymbol{\chi}^{(2)}$ for SHG can then be reduced to 4 nonzero and independent elements,[18] as follows:

$$\chi_{ZZZ}^{(2)}, \quad \chi_{ZXX}^{(2)} = \chi_{ZYY}^{(2)},$$
$$\chi_{XXZ}^{(2)} = \chi_{XZX}^{(2)} = \chi_{YYZ}^{(2)} = \chi_{YZY}^{(2)},$$
$$\chi_{XYZ}^{(2)} = \chi_{XZY}^{(2)} = -\chi_{YXZ}^{(2)} = -\chi_{YZX}^{(2)}.$$

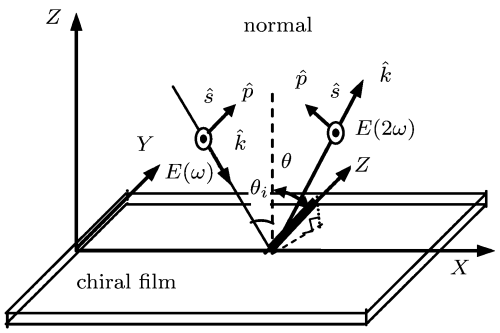


Fig. 1. Laser beam at frequency ω, incident on the sample at angle $\theta_{\rm inc}$, with surface normal being along the Z axis.

For isotropic surfaces of achiral molecules, there are an infinite number of mirror planes of symmetry perpendicular to the surface, thus the $\chi_{XYZ}^{(2)}$ elements vanish. For surfaces of chiral molecules, mirror planes of symmetry do not exist and all four elements are necessary to be used to describe the nonlinear behaviour of the surface.

2.1. Molecular polarizabilities of chiral molecule with tripod-like structure

The three-coupled-oscillator model is described in detail in Ref. [15]. It can be used for describing one kind of chiral molecule whose configuration looks like

a tripod due to the restriction of spatial structure between multiple groups, such as nitrobenzene derivatives, sulfur compound, and so on. We suggest using the three-coupled-oscillator model to describe such a kind of molecules as shown in Fig. 2. Cartesian coordinates with x, y, and z axes are fixed on the top of the tripod for describing their movement. (x, y, z) is the microscopic frame. The three oscillators have frequencies ω_{0i} and damping coefficients γ_i (i = 1, 2, 3) and they are coupled with each other through dipole–dipole interaction with small coupling parameters A_{ij} (i, j = 1, 2, 3). Positional vectors $\boldsymbol{r}_i$ (i = 1, 2, 3) of oscillators has an angle α_i with respect to the $x'O'y'$ plane (parallel to xOy plane). φ is the angle between two bonds. We assume that $\alpha_1 \approx \alpha_2 \approx \alpha_3 \approx \alpha$ for the convenience of calculation. At the rest position, the oscillators 1, 2, and 3 are located at $(\frac{1}{2}d\cot\alpha, -\frac{\sqrt{3}}{2}d\cot\alpha, -d)$, $(\frac{1}{2}d\cot\alpha, \frac{\sqrt{3}}{2}d\cot\alpha, -d)$, and $(-d\cot\alpha, 0, -d)$, respectively.[15] The relation between bond angle φ and α can be expressed as $\cos\alpha = (2\sqrt{3}/3)\sin(\varphi/2)$ approximately. We refer to a, b and c as the elongations of oscillators 1, 2, and 3 from their equilibrium positions.

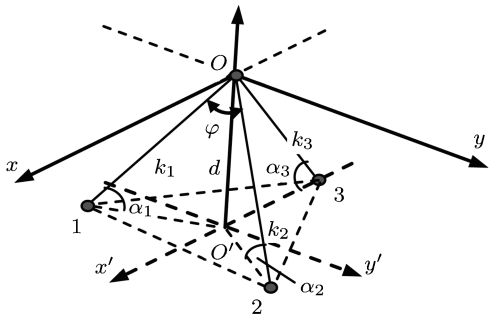


Fig. 2. Schematic diagram of three-coupled-oscillators model.

We suppose that the incident light is monochromatic light of frequency ω, so that the electric field around the oscillators can be written as $\boldsymbol{E}_i(\boldsymbol{r}, t) = \boldsymbol{E}_i(\boldsymbol{r})\exp(-\mathrm{i}\,\omega t) + \text{c.c.}$. The response of oscillators to the electric field contains not only the original frequency component, but also the second and third harmonic components. If only the second harmonic component is considered, the elongations of oscillators can be written as $a = a_1\mathrm{e}^{-\mathrm{i}\,\omega t} + a_2\mathrm{e}^{-\mathrm{i}\,2\omega t} + \text{c.c.}$, $b = b_1\mathrm{e}^{-\mathrm{i}\,\omega t} + b_2\mathrm{e}^{-\mathrm{i}\,2\omega t} + \text{c.c.}$, $c = c_1\mathrm{e}^{-\mathrm{i}\,\omega t} + c_2\mathrm{e}^{-\mathrm{i}\,2\omega t} + \text{c.c.}$.

The electric field around the coordinate origin can be expanded, with considering the spatial scattering of the electric field, into

$$E_{ij} = E_j + \frac{\partial E_j}{\partial x}x_i + \frac{\partial E_j}{\partial y}y_i + \frac{\partial E_j}{\partial z}z_i,$$
$$(i = 1, 2, 3; \quad j = x, y, z). \tag{5}$$

Considering the second-order nonlinear response of the system, the coupled equations of the oscillators along their respective oscillating directions can be written as[15]

$$D_1(2\omega)a_2 + A_{12}b_2 + A_{13}c_2 = \frac{q_1}{m_1}R_1a_1 - f_1a_1^2, \tag{6a}$$
$$D_2(2\omega)b_2 + A_{21}a_2 + A_{23}c_2 = \frac{q_2}{m_2}R_2b_1 - f_2b_1^2, \tag{6b}$$
$$D_3(2\omega)c_2 + A_{31}a_2 + A_{32}b_2 = \frac{q_3}{m_3}R_3c_1 - f_3c_1^2, \tag{6c}$$

where A_{ij} (i, j = 1, 2, 3) are the coefficients for weak coupling, $D_i(2\omega) = -4\omega^2 + \omega_{0i}^2 - 4\,\mathrm{i}\,\omega\gamma_i$, ($i$ = 1, 2, 3), f_i are the introduced anharmonic coefficients and can be estimated by $f_il^2 \approx \omega_{0i}^2 l$, where l is the elongation of oscillator from the equilibrium state,[19] and R_i is the linear combination of the electric field (E_jE_k) and its gradient ($E_j\partial E_l/\partial x_k$, $\partial E_k/\partial x_jE_l$) and their coefficients are related to the direction cosines of the field in the direction of oscillation.

The second-order nonlinear electric dipole moment can be expressed as

$$p_i^{(2)}(2\omega) = \varepsilon_0\beta_{ijk}^{(2)}E_j(\omega)E_k(\omega) + 2\varepsilon_0\tilde{\beta}_{ijkl}^{\mathrm{eeq}}E_j(\omega)\nabla_kE_l(\omega). \tag{7}$$

The molecular electric dipole moment can be described by the following equation:

$$\boldsymbol{p} = \sum_j q_j\boldsymbol{r}_j, \tag{8}$$

where $\boldsymbol{r}_j$ is the position vector of the oscillator, which is related to the effect of electric field on three oscillators. Therefore, the molecular electric dipole moment in electric field can be expanded into

$$p_i = p_{i0} + p_i^{(1)}\exp(-\mathrm{i}\,\omega t) + p_i^{(2)}\exp(-\mathrm{i}\,2\omega t) + \ldots + \text{c.c.}, \quad (i = x, y, z), \tag{9}$$

where p_{i0} is the molecular intrinsic electric dipole moment; $p_i^{(1)}(\omega)$ and $p_i^{(2)}(2\omega)$ are the linear and the second-order nonlinear polarizabilities of the molecule, respectively. On the basis of Eqs. (5)–(9), we can obtain the hyperpolarizabilities $\beta_{ijk}^{(2)}$of chiral molecules with a tripod-like structure (see Appendix).

We derive the nonvanishing-independent components of $\chi_{IJK}^{\mathrm{eee}}(2\omega)$ from Eq. (4) as follows:

$$\chi^{(2)}_{ZZZ} = \frac{N\cos\theta}{2}[(2\beta^{(2)}_{xxz} + 2\beta^{(2)}_{yyz} + \beta^{(2)}_{zxx} + \beta^{(2)}_{zyy})\sin^2\theta + 2\beta^{(2)}_{zzz}\cos^2\theta], \tag{10a}$$

$$\chi^{(2)}_{ZXX} = \frac{N\cos\theta}{4}[2(-\beta^{(2)}_{xxz} - \beta^{(2)}_{yyz} + \beta^{(2)}_{zzz})\sin^2\theta + (1+\cos^2\theta)(\beta^{(2)}_{zxx} + \beta^{(2)}_{zyy})], \tag{10b}$$

$$\chi^{(2)}_{XXZ} = \frac{N\cos\theta}{4}[2(\beta^{(2)}_{xxz} + \beta^{(2)}_{yyz})\cos^2\theta - (\beta^{(2)}_{zxx} + \beta^{(2)}_{zyy} - 2\beta^{(2)}_{zzz})\sin^2\theta], \tag{10c}$$

$$\chi^{(2)}_{XYZ} = \frac{N}{4}(2\cos^2\theta - \sin^2\theta)(\beta^{(2)}_{xyz} - \beta^{(2)}_{yxz}), \tag{10d}$$

where θ is Euler angle (namely, polar angle with respect to the surface normal, the Z axis in the laboratory frame, see Fig. 1).

For an isotropic surface, $\boldsymbol{\chi}^{(2)}$ can be separated into chiral items $\chi^{(2)}_{\rm chiral}$ and achiral items $\chi^{(2)}_{\rm achiral}$. The chiral items $\chi^{(2)}_{\rm chiral}$, such as $\chi^{(2)}_{YXZ}$ and $\chi^{(2)}_{XYZ}$, are only allowed for chiral surface and will change their signs when the surface with an enantiomer changes into the surface with an opposite enantiomer. The achiral items $\chi^{(2)}_{\rm achiral}$, such as $\chi^{(2)}_{ZZZ}, \chi^{(2)}_{ZXX}$, and $\chi^{(2)}_{XZX}$, are allowed for the surface with any molecules, including chiral ones.

2.2. Second harmonic generation circular dichroism

For circularly polarized light incident on a monolayer consisting of the chiral molecules, the SHG efficiency is shown to depend strongly on the handedness of the circularly polarized excitation beam, which is in contrast to ordinary CD effect, where the difference in absorbance between the left- and the right-handed circularly polarized light is much larger because SHG-CD is electric dipole allowed. Experiments show that the SHG-CD in nonlinear optics is the technique most sensitive to chirality of surface and interface.[8] Moreover, the SHG-CD is bound up with molecular structure. The SHG-CD therefore is broadly applied to the detection of chirality of thin films.

For circularly polarized fundamental beams, $E_p(\omega) = \pm \mathrm{i}\, E_s(\omega)$ and the intensity of the second-harmonic field is obtained from Eq.(2) as

$$I(2\omega) = |-f + g \pm \mathrm{i}\, h|^2\, I^2(\omega), \tag{11}$$

where the upper and lower signs (i.e., signs + and – of symbol±) correspond, respectively, to the right and the left circular polarizations, and $I(\omega) = |E_s(\omega)|^2$. Equation (11) shows that the responses to the left and the right circularly polarized light can be different only if neither (f-g) nor h is zero. For surfaces that are isotropic in the surface plane, (f–g) and h are nonvanishing only when the surface is chiral. The SHG-CD effects can be expressed as

$$\Delta I(2\omega) = I_{\rm L}(2\omega) - I_{\rm R}(2\omega) \propto [{\rm Im}(h^* f) + {\rm Im}(g^* h)]I^2(\omega), \tag{12}$$

where $I_{\rm L}$ and $I_{\rm R}$ denote the left- and the right-handed circularly polarized beams, respectively. For an isotropic surface, it is only related to the four independent components of $\boldsymbol{\chi}^{(2)}$. It is clear from Eq. (12) that h and f, g must differ in phase for the circular-difference effect to occur.

The coefficients f, g and h are functions of the macroscopical polarizability $\chi^{(2)}_{IJK}$ and the incident angle θ_{inc} in equations (12). They can be split into the s and the p components corresponding to the s- and the p-polarized components of the second-harmonic field.[17,20,21] In the reflected direction, their expressions based on the three-coupled-oscillator model can be written as

$$\begin{aligned}
f_s &= 2\chi^{\rm eee}_{xyz}\sin\theta_{\rm inc}\cos\theta_{\rm inc},\\
g_s &= 0, \quad h_s = 2\chi^{\rm eee}_{xxz}\sin\theta_{\rm inc},\\
f_p &= \sin\theta_{\rm inc}(\chi^{\rm eee}_{zzz}\sin^2\theta_{\rm inc} + \chi^{\rm eee}_{zxx}\cos^2\theta_{\rm inc}\\
&\quad - 2\chi^{\rm eee}_{xxz}\cos^2\theta_{\rm inc}),\\
g_p &= \chi^{\rm eee}_{zxx}\sin\theta_{\rm inc},\\
h_p &= -\chi^{\rm eee}_{xyz}\sin\theta_{\rm inc}\cos\theta_{\rm inc}.
\end{aligned} \tag{13}$$

In these equations, subscripts s and p correspond to the signals detected being s- and p-polarized respectively. So, for the case of surface with tripod-like chiral molecules in the direction of reflected light,

$$\Delta I_s(2\omega) \propto {\rm Im}(\chi^{(2)*}_{XXZ}\chi^{(2)}_{XYZ}) \tag{14a}$$

for s-polarization, and

$$\begin{aligned}
\Delta I_p(2\omega) \propto &[{\rm Im}(-\chi^{(2)*}_{XYZ})(\chi^{(2)}_{ZZZ}\sin^2\theta_{\rm inc}\\
&+ \chi^{(2)}_{ZXX}\cos^2\theta_{\rm inc} - 2\chi^{(2)}_{XXZ}\cos^2\theta_{\rm inc})\\
&+ {\rm Im}(-\chi^{(2)}_{XYZ}\chi^{(2)*}_{ZXX})]
\end{aligned} \tag{14b}$$

for p-polarization.

Equations (14a) and (14b) imply that the second-harmonic generation has different responses to the

left- and the right-hand circularly polarized fundamental fields, and also that chiral tensor component $\chi^{(2)}_{XYZ}$ influences the SHG-CD effect. The tensor components containing three direction elements: $\chi^{(2)}_{XYZ}$, $\chi^{(2)}_{YXZ}$ and $\chi^{(2)}_{ZXY}$, are designated by the name of chiral tensor components. Among the components of $\boldsymbol{\chi}^{(2)}$, chiral component $\chi^{(2)}_{XYZ}$ is allowed only by the chirality of the surface, whereas the other components are allowed under arbitrary conditions. Therefore SHG-CD is sensitive to chirality because of the presence of chiral tensor component $\chi^{(2)}_{XYZ}$.

In the three-coupled-oscillator model, there is no component of interaction between electric-dipole and magnetic-dipole because we suppose that the three oscillators move along their bond directions respectively, the magnetic-induction field is zero. Correspondingly, macroscopic second-order susceptibility $\chi^{\mathrm{eem}}_{ijk}(0;-\omega,\omega)$ vanishes, which leads to $g_s = 0$ in the s-polarized component of the second-harmonic field in Eq. (13). So, in this model, the SHG-CD effect occurs only within the electric dipole approximation.

The origination of chirality is related to the microscopic structure of chiral molecule. From Eq. (10), one can see that the achiral tensor $\boldsymbol{\beta}^{(2)}$ has no contribution to the chiral tensor $\boldsymbol{\chi}^{(2)}$, similarly, the chiral tensor $\boldsymbol{\beta}^{(2)}$ has no contribution to the achiral tensor $\boldsymbol{\chi}^{(2)}$ either. Therefore, for an isotropic surface, the chirality at molecular level consequentially leads to the presence of nonvanishing chiral component $\chi^{(2)}_{\mathrm{chiral}}$, which has been experimentally proved.[18,22] According to the discussion above, the presence of a nonzero $\chi^{(2)}_{XYZ}$ is crucial to the observation of SHG-CD effect.

From Eqs. (11) and (13), the intensity of the second-harmonic field can be written as

$$I_s(2\omega) \propto |-\chi^{\mathrm{eee}}_{XYZ}\cos\theta_{\mathrm{inc}} \pm \mathrm{i}\,\chi^{\mathrm{eee}}_{XXZ}|^2\, I^2(\omega), \tag{15a}$$

$$I_p(2\omega) \propto |(\chi^{\mathrm{eee}}_{ZXX} - \chi^{\mathrm{eee}}_{ZZZ})\sin^2\theta_{\mathrm{inc}} + 2\chi^{\mathrm{eee}}_{XXZ}\cos^2\theta_{\mathrm{inc}} \mp \mathrm{i}\,\chi^{\mathrm{eee}}_{XYZ}\cos\theta_{\mathrm{inc}}|^2 I^2(\omega), \tag{15b}$$

where the upper and lower signs represent the left- and the right-hand circularly polarized fundamental light, respectively.

For measurements of either the s- or the p-polarized second-harmonic light, the use of Eqs. (1), (11) and (12) gives

$$I_{\mathrm{SHG-CD}} = \frac{4[\mathrm{Im}(g^*h) + \mathrm{Im}(h^*f)]}{|f|^2 + |g|^2 + |h|^2 - 2\,\mathrm{Re}(f^*g)}, \tag{16}$$

which can be used to predict the strength of the SHG-CD effect. A more complicated expression is required to model the SHG-CD effect in the total intensity. Equation (16) shows that a phase difference must exist between h and f or g for the SHG-CD effect to exist, where a 90° phase difference is an optimal value.

Since the dichroism of the second harmonic response requires significant imaginary component of the $\boldsymbol{\chi}^{(2)}$ element, the effect should be observable only near resonance. The spectral properties provide important information about the nature of the species and the electronic states producing the SHG, and the SHG-CD spectral information is given in Fig. 3. The differences in intensity between the left- and the right-hand circularly-polarized beams are given in Fig. 4. Spectral characters of SHG from tripod-like chiral molecular films for the left- and the right-handed circularly polarized incident light are given in Fig. 5.

3. Numerical simulation and analysis

SHG-CD spectrum can be obtained from Eq. (16). We simulate numerically the relation between SHG-CD and second-harmonic wavelength, namely SHG-CD spectrum, at a certain incident light intensity. We choose the equilibrium elongation l to be 0.116 nm, and the molecular surface density N to be 4.0×10^{26} m^{-2}. The plots of SHG-CD versus second harmonic wavelength for different chiralities are given in Fig. 3 on condition that the resonance centre frequency ω_0 is 5.24×10^{15} Hz, the damping coefficients γ_i is $(1/10)\omega_{0i}$, incident angle of light wave θ_{inc} is $\pi/4$, and bond angle of molecule is $\pi/2$.

The s- and the p-polarized SHG-CD spectra in the reflective light are shown in Figs. 3(a) and 3(b), respectively. Among the curves in the figures, curve A is corresponding to the symmetric molecular structure, i.e. no chirality, while curves B, C and D are corresponding to dissimilar asymmetric molecular structures respectively. The curves A–D have the following chiral components: $\omega_{01}/\omega_{02} = 1$, 1.06, 1.09, 1.16; $\omega_{02}/\omega_{03} = 1$, 1.06, 1.08, 1.14; $\omega_{03}/\omega_{01} = 1$, 0.89, 0.85, 0.76.

From Fig. 3, we know that when three oscillators are the same (i.e., no chiralities), the circular dichroism s- and p-polarized components $I^s_{\mathrm{SHG-CD}}$ and $I^p_{\mathrm{SHG-CD}}$ are both zero, in other words, there is no SHG-CD effect (see curve A in Fig. 3). This phenomenon shows that the SHG-CD effect occurs only in thin film with chiral molecules. The SHG-CD spectrum changes distinctly with chirality of molecule, for

example, curve B is the case where two oscillators are the same, and curves C and D have three dissimilar oscillators in Fig. 3. There are only positive branches of SHG-CD on curve B, and there are both positive and negative branches of SHG-CD in curves C and D, which indicates the influence of molecular structure on SHG-CD. Hence, the SHG-CD spectrum can give information about molecular structure. Figure 3 also shows that the stronger the chirality of molecule is, the more prominent the SHG-CD effect will be, such as curve D. This suggests that the chiral contribution dominates the SHG-CD and indicates the SHG-CD effect is sensitive to chirality, which makes it a sensitive technique to detect chirality accordingly.

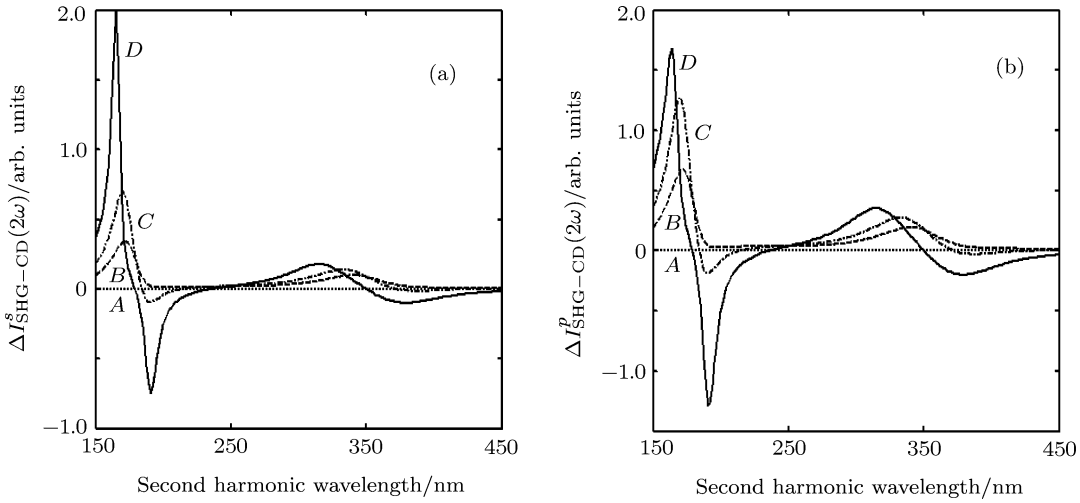


Fig. 3. SHG-CD spectra under the condition of different chiralities (from A to D, chiral components: $\omega_{01}/\omega_{02} = 1, 1.06, 1.09, 1.16$; $\omega_{02}/\omega_{03} = 1, 1.06, 1.08, 1.14$; $\omega_{03}/\omega_{01} = 1, 0.89, 0.85, 0.76$), where panel (a) is for the s-polarized beam case and panel (b) is for the p-polarized beam case.

The SHG-CD spectral information given in Fig. 3 shows the characteristic of absorbable band and positive or negative circular dichroism in the whole area of wavelength. The values of SHG-CD and absorbable wavelength ($\lambda_{\max}$) are varying with the changing of molecular chirality. But absorbable wavelength at $\lambda_{\max} = 190$ nm is invariable while the s- and the p-polarized SHG-CD spectra change with molecular chirality. In the area of wavelengths 150–230 nm there occurs a strong absorbable section, but in 280–400 nm there appears a weak absorbable section. Peak value of p-polarized SHG-CD is greater than that of s-polarized in negative circular dichroism, but such a rule does not exist in the positive circular dichroism.

Increase in SHG-CD ratio reaches high values of up to $I^s_{\rm SHG-CD} = 1.99$ and $I^p_{\rm SHG-CD} = 1.6$ around second harmonic wavelength 165 nm from our calculation, where chiral components are $\omega_{01}/\omega_{02} = 1.16$, $\omega_{02}/\omega_{03} = 1.14$, and $\omega_{03}/\omega_{01} = 0.76$.

The differences in intensity between the left- and the right-hand circularly polarized beams, $\Delta I(2\omega) = I_{\rm L}(2\omega) - I_{\rm R}(2\omega)$ versus second-harmonic wavelength under condition of different chiralities, namely $\Delta I(2\omega)$ spectrum, can be obtained from Eq. (14). Figures 4(a) and 4(b) show the spectral dependences of $\Delta I_s(2\omega)$ and $\Delta I_p(2\omega)$, respectively, where $\Delta I_s(2\omega)$ is corresponding to the s-polarized beam and $\Delta I_p(2\omega)$ is corresponding to the p-polarized beam. In Figs. 4(a) and 4(b), curve A demonstrates that $\Delta I(2\omega) = 0$ when all the three oscillators are the same, which means that the molecular configuration is symmetric (viz. no chirality); curve B corresponds to the case where two oscillators have the same chiral relation (ω_{01}/ω_{02}=1.06; ω_{02}/ω_{03}=1.06; ω_{03}/ω_{01}=0.89); and curve C corresponds to the case where three oscillators are dissimilar (ω_{01}/ω_{02}=1.06; ω_{02}/ω_{03}=1.14; ω_{03}/ω_{01}=0.76). It can be seen from Fig. 4 that spectra of $\Delta I_s(2\omega)$ and $\Delta I_p(2\omega)$ possess almost the same characteristics except their intensities. This fact shows that chiral component $\chi^{(2)}_{XXZ}$ plays an important role in $\Delta I_s(2\omega)$ and $\Delta I_p(2\omega)$ spectra, thus we can obtain some information about chiral configuration of molecules from $\Delta I(2\omega)$ spectrum. From our further research, we also find that the first term in Eq. (14b) exerts an main effect on the spectrum of $\Delta I_p(2\omega)$, which implies that $\Delta I_p(2\omega)$ is sensitive to chirality, too.

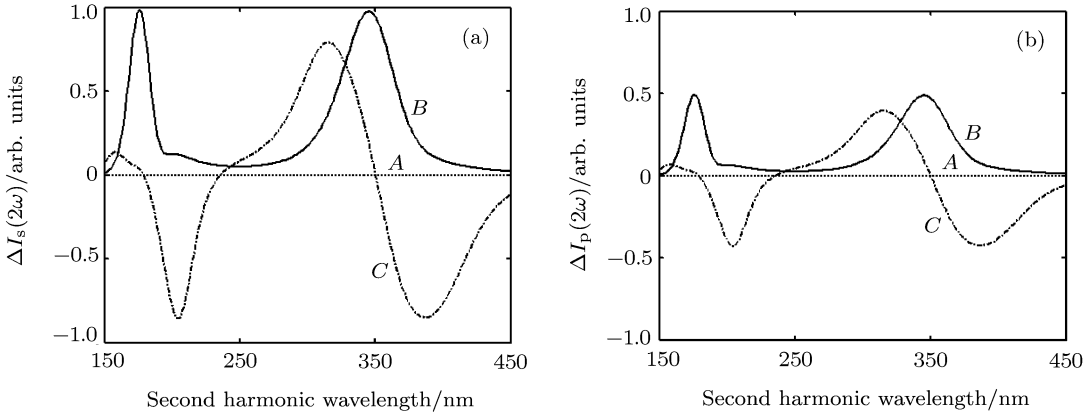


Fig. 4. Spectral dependence of the circular dichroism $\Delta I(2\omega) = I_L(2\omega) - I_R(2\omega)$ of SHG under condition of different chirality (from A to C, chiral components: $\omega_{01}/\omega_{02} = 1, 1.06, 1.16$; $\omega_{02}/\omega_{03} = 1, 1.06, 1.14$; $\omega_{03}/\omega_{01} = 1, 0.89, 0.76$), where panel (a) is for s-polarized beam case and panel (b) is for p-polarized beam case.

Since the dichroism of the second harmonic response requires significant imaginary component of the $\boldsymbol{\chi}^{(2)}$ element, the effect should be observed only near resonance. The spectral properties provide the important information about the nature of the species and the electronic states producing the SHG. The s- and the p-components of the SHG signal from thin film of chiral molecules are collected as functions of wavelength and incident polarization. The data for the left and the right circularly polarized excitations are shown in Fig. 5, on the assumption that the incident light intensity is certain, incident angle is 45°, chiral relations are ω_{01}/ω_{02}=1.16, ω_{02}/ω_{03}=1.14, and ω_{03}/ω_{01}=0.76. Figure 5(a) shows corresponds to s-polarized beam case and Fig. 5(b) corresponds to p-polarized beam case, where solid line represents the left circular polarized incident light while dash line represents the right circular polarized incident light. There is a strong preference for right circularly polarized light in the area of second harmonic wavelengths 145–179 nm, whose magnitude varies with wavelength. Preference for the left or the right circularly polarized light changes near the second harmonic wavelength 179 nm.

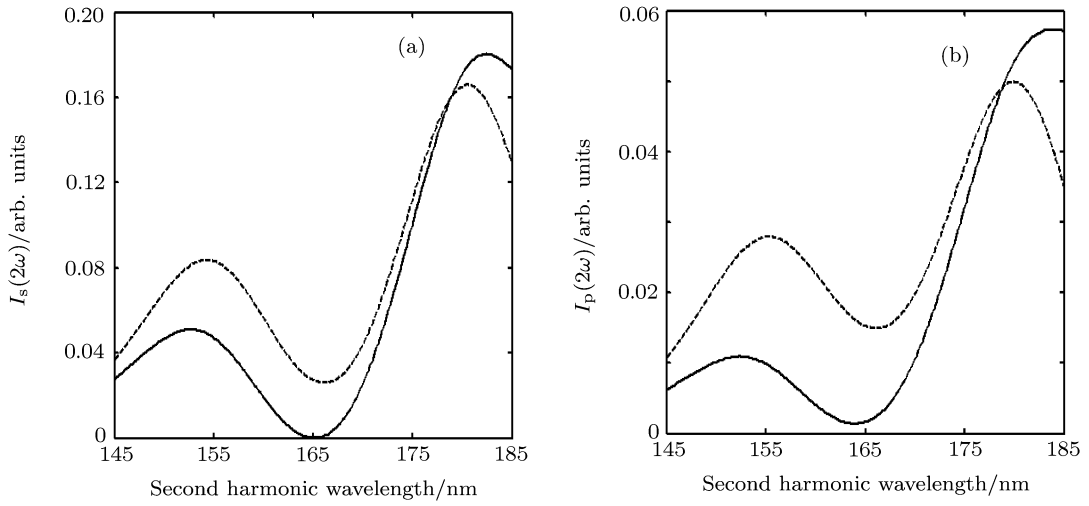


Fig. 5. Spectral dependences of SHG for left (solid line) and right (dash line) circularly polarized incident light, where panel (a) is for s-polarized beam case and panel (b) is for p-polarized beam case.

4. Conclusions

In this paper, we derive the hyperpolarizabilities of the tripod-like chiral molecules under the condition of second harmonic generation and presente the expression of SHG-CD for tripod-like chiral molecular films based on the three-coupled-oscillator model. We simulate numerically the relation between SHG-CD and molecular

microscopic parameters when incident light intensity is determinate. The influence of chiral parameters on SHG-CD spectrum in tripod-like chiral molecular films and intensity of SHG spectrum in reflection are also investigated. On the chiral condition $\omega_{01}/\omega_{02} = 1.16$, $\omega_{02}/\omega_{03} = 1.14$, $\omega_{03}/\omega_{01} = 0.76$, we can obtain the SHG-CD ratios which are as high as $I^{s}_{\mathrm{SHG-CD}} = 1.99$ and $I^{p}_{\mathrm{SHG-CD}} = 1.6$ around the second harmonic wavelength 165nm from our calculation. The fact shows that SHG-CD is a sensitive method of detecting chirality, which is consistent with the conclusion given by Byers *et al.*[8]

Our research indicates that the second order nonlinear optical effects are in direct proportion to chirality, thus SHG-CD is derived from chiral molecular structure. It is further illuminated that the SHG-CD is a sensitive method of detecting chirality. In addition, compared with conventional researches on the nonlinear processes of chiral media, this base-on-molecular-model method is not only more intuitional but also more accurate, and it gives the information about molecular structure and provides a new theoretical basis for marking the tripod-like chiral molecular media.

Appendix

$$
\begin{aligned}
\beta^{(2)}_{xyz} &= -\frac{\sqrt{3}q^3\sin\alpha\cos^2\alpha}{4\varepsilon_0 m^2}\Bigg[\left(\frac{f_1}{D_1(2\omega)D_1^2(\omega)}-\frac{f_2}{D_2(2\omega)D_2^2(\omega)}\right)\left(1-\frac{A_{13}(D_3(2\omega)-2D_3(\omega))}{D_3(2\omega)D_3(\omega)}\right)\\
&\quad+\frac{A_{12}}{D_2(2\omega)D_1(2\omega)}\left(\frac{f_2}{D_2^2(\omega)}-\frac{f_1}{D_1^2(\omega)}\right)-\frac{2A_{13}f_3(D_1(\omega)-D_2(\omega))}{D_3(2\omega)D_3^2(\omega)D_2(\omega)D_1(\omega)}\Bigg],\\
\beta^{(2)}_{xxz} &= \frac{q^3\sin\alpha\cos^2\alpha}{4\varepsilon_0 m^2}\Bigg[\left(\frac{f_1}{D_1(2\omega)D_1^2(\omega)}+\frac{f_2}{D_2(2\omega)D_2^2(\omega)}\right)\left(1+\frac{A_{13}(D_3(2\omega)+2D_3(\omega))}{D_3(2\omega)D_3(\omega)}\right)\\
&\quad+\frac{4f_3}{D_3(2\omega)D_3^2(\omega)}-\frac{A_{12}}{D_2(2\omega)D_1(2\omega)}\left(\frac{f_1(2D_2(2\omega)+D_2(\omega))}{D_2(\omega)D_1^2(\omega)}+\frac{f_2(2D_1(2\omega)+D_1(\omega))}{D_1(\omega)D_2^2(\omega)}\right)\\
&\quad-\frac{2A_{13}f_3}{D_3(2\omega)D_3^2(\omega)}\left(\frac{2D_2(2\omega)-D_2(\omega)}{D_2(2\omega)D_2(\omega)}+\frac{2D_1(2\omega)-D_1(\omega)}{D_1(2\omega)D_1(\omega)}\right)\Bigg],\\
\beta^{(2)}_{yxz} &= \frac{\sqrt{3}q^3\sin\alpha\cos^2\alpha}{8\varepsilon_0 m^2}\Bigg[\left(\frac{f_2}{D_2^2(\omega)D_2(2\omega)}-\frac{f_1}{D_1^2(\omega)D_1(2\omega)}\right)\left(1+\frac{A_{13}}{D_3(\omega)}\right)\\
&\quad-\frac{A_{12}}{D_2(2\omega)D_1(2\omega)}\left(\frac{f_1(D_2(\omega)-2D_2(2\omega))}{D_2(\omega)D_1^2(\omega)}+\frac{f_2(2D_1(2\omega)-D_1(\omega))}{D_2^2(\omega)D_1(\omega)}\right)-\frac{2A_{13}f_3(D_2(2\omega)-D_1(2\omega))}{D_3^2(\omega)D_3(2\omega)D_2(2\omega)D_1(2\omega)}\Bigg],\\
\beta^{(2)}_{yyz} &= \frac{3q^3\sin\alpha\cos^2\alpha}{8\varepsilon_0 m^2}\Bigg[\left(\frac{f_1}{D_1(2\omega)D_1^2(\omega)}+\frac{f_2}{D_2(2\omega)D_2^2(\omega)}\right)\left(1-\frac{A_{13}}{D_3(\omega)}\right)\\
&\quad+\frac{A_{12}}{D_2(2\omega)D_1(2\omega)}\left(\frac{f_1}{D_1^2(\omega)}+\frac{f_2}{D_2^2(\omega)}\right)\Bigg],\\
\beta^{(2)}_{zxx} &= \frac{q^3\sin\alpha\cos^2\alpha}{4\varepsilon_0 m^2}\Bigg[\left(\frac{f_1}{D_1(2\omega)D_1^2(\omega)}+\frac{f_2}{D_2(2\omega)D_2^2(\omega)}\right)\left(1+\frac{A_{13}(4D_3(2\omega)-D_3(\omega))}{D_3(2\omega)D_3(\omega)}\right)\\
&\quad-\frac{A_{12}}{D_2(2\omega)D_1(2\omega)}\left(\frac{f_1(D_2(\omega)+2D_2(2\omega))}{D_2(\omega)D_1^2(\omega)}+\frac{f_2(D_1(\omega)+2D_1(2\omega))}{D_2^2(\omega)D_1(\omega)}\right)\\
&\quad+\frac{4f_3}{D_3(2\omega)D_3^2(\omega)}\left(1+A_{13}\left(\frac{(D_1(2\omega)-D_1(\omega))}{D_1(2\omega)D_1(\omega)}+\frac{(D_2(2\omega)-D_2(\omega))}{D_2(2\omega)D_2(\omega)}\right)\right)\Bigg],\\
\beta^{(2)}_{zyy} &= \frac{3q^3\sin\alpha\cos^2\alpha}{4\varepsilon_0 m^2}\Bigg[\left(\frac{f_1}{D_1(2\omega)D_1^2(\omega)}+\frac{f_2}{D_2(2\omega)D_2^2(\omega)}\right)\left(1-\frac{A_{13}}{D_3(2\omega)}\right)\\
&\quad+\frac{A_{12}}{D_2(2\omega)D_1(2\omega)}\left(\frac{f_1(2D_2(2\omega)-D_2(\omega))}{D_2(\omega)D_1^2(\omega)}+\frac{f_2(2D_1(2\omega)-D_1(\omega))}{D_2^2(\omega)D_1(\omega)}\right)\Bigg],\\
\beta^{(2)}_{zzz} &= \frac{q^3\sin^3\alpha}{\varepsilon_0 m^2}\Bigg[\left(\frac{f_1}{D_1(2\omega)D_1^2(\omega)}+\frac{f_2}{D_2(2\omega)D_2^2(\omega)}\right)\left(1-\frac{A_{13}(D_3(\omega)+2D_3(2\omega))}{D_3(2\omega)D_3(\omega)}\right)\\
&\quad+\frac{f_3}{D_3(2\omega)D_3^2(\omega)}-\frac{D_1(\omega)+2D_1(2\omega)}{D_1(2\omega)D_1(\omega)}\left(\frac{A_{13}f_3}{D_3(2\omega)D_3^2(\omega)}+\frac{A_{12}f_2}{D_2(2\omega)D_2^2(\omega)}\right)
\end{aligned}
$$

$$-\frac{D_2(\omega)+2D_2(2\omega)}{D_2(2\omega)D_2^{(}\omega)}\left(\frac{A_{12}f_1}{D_1(2\omega)D_1^2(\omega)}+\frac{A_{13}f_3}{D_3(2\omega)D_3^2(\omega)}\right)\Bigg],$$

with $A_{12}=k_{12}(\frac{3}{2}\cos^2\alpha-1)/m$, $A_{13}=k_{13}(\frac{1}{2}\cos^2\alpha-1)/m$, and $D_i(\omega)=-\omega^2+\omega_{0i}^2-2\,\mathrm{i}\,\omega\gamma_i$ $(i=1,\,2,\,3)$.

References

[1] Ostroverkhov V, Ostroverkhova O, Petschek R G and Singer K D 2000 *Chem. Phys.* **257** 263

[2] Ledoux and Zyss J 2002 *C. R. Physique* **3** 407

[3] Champagne B, Fischer P and David Buckingham A 2000 *Chem. Phys. Lett.* **331** 83

[4] Davis D, Sreekumar K and Pati S K 2005 *Synthetic Metals* **155** 384

[5] Petralli-Mallow T, Wong T M, Byers J D, Yee H I and Hicks J M 1993 *J. Phys. Chem.* **97** 1383

[6] Giffarda M, Merciera N, Mabon G, Phu X N, Sylla M, Delhaès P, Soscún H, CastellanoO, Hernández J, Rodríguez L, Marcano A and Yartsev V 2005 *Microelectronics Journal* **36** 933

[7] Sioncke S, Verbiest T and Persoons A 2003 *Materials Science and Engineering* R **42** 115

[8] Byers J D, Yee H I, Petralli-Mallow T and Hicks J M 1994 *Phys. Rev.* B **49** 14643

[9] Manaka T, Tamura R and Iwamoto M 2006 *Colloids and Surfaces* A: *Physicochem. Eng. Aspects.* **284** 409

[10] Araoka F, Ha N Y, Kinoshita Y, Park B, Wu J W and Takezoe H 2005 *Phys. Rev. Lett.* **94** 137801

[11] Fischer P and Albrecht A C 2002 *Laser Physics: Nonlinear and Quantum Optics* **12** 1177

[12] Maki J J and Persoons A 1996 *J. Chem. Phys.* **104** 9340

[13] Hache F, Mesnil H and Schanne-Klein M C 2001 *J. Chem. Phys.* **115** 6707

[14] Mesnil H, Schanne-Klein M C and Hache F 2002 *Phys. Rev.* A **66** 013802

[15] Wang X O, Li J Q and Li C F 2005 *Chem. Phys.* **320** 37

[16] Wang X O, Li J Q and Li C F 2006 *Chin. Phys.* **15** 2623

[17] Kauranen M, Verbiest T, Maki J J and Persoons A 1994 *J. Chem. Phys.* **101** 8193

[18] Mazely T L and Hetherington III W M 1987 *J. Chem. Phys.* **86** 3640

[19] Boyd R W 1992 *Nonlinear Optic* (San Diego: Academic Press) p27

[20] Maki J J, Kauranen M and Persoons A 1995 *Phys. Rev.* B **51** 1425

[21] Schanne-Klein M C, Hache F, Roy A, Flytzanis C and Payrastre C 1998 *J. Chem. Phys.* **108** 9436

[22] Byers J D, Yee H I and Hicks J M 1994 *J. Chem. Phys.* **101** 6233